EJN European Journal of Neuroscience

FENS Federation of European Neuroscience Societies

European Journal of Neuroscience, Vol. 40, pp. 3653–3662, 2014 doi:10.1111/ejn.12736

MOLECULAR AND SYNAPTIC MECHANISMS

High-frequency electrical stimulation suppresses cholinergic accumbens interneurons in acute rat brain slices through $GABA_B$ receptors

Yijing Xie,[1,2] Tjitske Heida,[3] Jan Stegenga,[3] Yan Zhao,[3] Andreas Moser,[4] Volker Tronnier,[2,5] Thomas J. Feuerstein[6,7] and Ulrich G. Hofmann[1,2,8]

[1]Neuroelectronic Systems, Department of Neurosurgery, University Medical Center Freiburg, 79108 Freiburg, Germany
[2]Graduate School for Computing in Medicine and Life Sciences, University of Lübeck, Lübeck, Germany
[3]Biomedical Signals and Systems, University of Twente, Enschede, The Netherlands
[4]Clinic for Neurology, University of Lübeck, Lübeck, Germany
[5]Clinic for Neurosurgery, University of Lübeck, Lübeck, Germany
[6]Freiburg Institute for Advanced Studies (FRIAS), University of Freiburg, Freiburg, Germany
[7]Section of Clinical Neuropharmacology, Department of Neurosurgery, University Medical Center Freiburg, Freiburg, Germany
[8]Institute for Signal Processing, University of Lübeck, Lübeck, Germany

Keywords: γ-aminobutyric acid, acetylcholine interneuron, deep brain stimulation, high-frequency electrical stimulation, nucleus accumbens, obsessive-compulsive disorder

Abstract

The nucleus accumbens is selected as a surgical target in deep brain stimulation for treating refractory obsessive-compulsive disorder (OCD). One of the therapeutic benefits of this procedure is that the abnormal hyper-functioning prefrontal cortex of patients with OCD is restored during stimulation. One hypothesis regarding the mechanism of deep brain stimulation is that the neuronal electrophysiological properties are directly altered by electrical stimulation; another hypothesis assumes that the stimulation induces selective neuron transmitter release, such as γ-aminobutyric acid (GABA). In this study, we used multi-electrode arrays with electrode size of 40 × 40 μm to record electrophysiological signals from the large nucleus accumbens neurons in acute rat brain slices while applying electrical stimulation simultaneously. We revealed that high-frequency stimulation (HFS, 140 Hz) suppressed the spontaneous neuronal firing rate significantly, whereas low-frequency stimulation (LFS, 10 Hz) did not. Both HFS and LFS have no effect on neuronal firing pattern or on neuronal oscillation synchrony. $GABA_B$ receptor antagonism reversed the HFS-provoked neuronal inhibition, whereas $GABA_A$ receptor blockade failed to affect it. The recorded neurons were pharmacologically identified to be cholinergic interneurons. We propose that HFS has a direct suppressive effect on the identified accumbal acetylcholine (ACh) interneurons by enhancing GABA release in the stimulated region. Potentially, suppressed ACh interneurons decrease the disinhibiting function of medium-sized spiny neurons in the striato-thalamo-cortical circuit. This finding might give an indication of the mechanism of the therapeutic effect of HFS in nucleus accumbens on restoring the abnormal hyperactive prefrontal cortex status in OCD.

Introduction

Deep brain stimulation (DBS) has been introduced to reduce motor symptoms in neurodegenerative diseases (e.g. Parkinson's disease, essential tremor and dystonia). DBS delivers high-frequency (130–185 Hz) electrical pulses with variable intensities to the target brain area through chronically implanted electrodes (Benabid *et al.*, 1991). DBS is currently proposed as an effective surgical intervention for various dysfunctional syndromes, such as epilepsy, depression and obsessive-compulsive disorder (OCD) (Tronnier & Fogel, 2000; Gross, 2004; Huff *et al.*, 2010). Although the exact pathophysiological process underlying OCD has not been fully established, brain areas purportedly involved in OCD are the orbitofrontal cortex, dorsal/ventral striatum, thalamus and ventral globus pallidus (Aouizerate *et al.*, 2004b; Rauch *et al.*, 2006). The currently postulated neural circuit dysfunction of OCD is orbitofrontal cortex hyperactivity and failure of ventral striatum-mediated thalamofrontal inhibition (Lozano & Lipsman, 2013). Drug-resistant patients are candidates for DBS. The nucleus accumbens (NAcc), as part of the ventral striatum, is chosen as the target of DBS for refractory OCD, based on clinical observations of DBS outcomes as well as anatomical and pathophysiological data (Sturm *et al.*, 2003; Aouizerate *et al.*, 2004a; Kuhn *et al.*, 2009).

Correspondence: Professor Dr U. G. Hofmann, [1]Neuroelectronic Systems, as above.
E-mail: ulrich.hofmann@coregen.uni-freiburg.de

Y.X. and T.H. contributed equally to this study.

Received 16 April 2014, revised 12 August 2014, accepted 25 August 2014

Unfortunately, the mechanisms of action of high-frequency stimulation (HFS) underlying the clinical results are still not fully understood. The current hypothesis on the pathophysiological level is that spike initiation at the neuronal somata is strongly altered resulting in inhibiting action potentials, while the efferent axons to the stimulated area are probably excited (McIntyre *et al.*, 2004; Benabid *et al.*, 2005; Kringelbach *et al.*, 2007). Furthermore, inhibited neuronal activities at the stimulation site may occur due to either depression of voltage-gated currents (Beurrier *et al.*, 2001), inhibition of intrinsic and synaptically mediated activities (Filali *et al.*, 2004), or selective local γ-aminobutyric acid (GABA) release (Feuerstein *et al.*, 2011). In basal ganglia-related motor disorders, such as Parkinson's disease and dystonia, the abnormal subthalamic nucleus and subthalamic nucleus–internal globus pallidus oscillation synchrony are strongly related to the pathological symptoms, and the synchrony can be modified by electrical stimulation (Bergman *et al.*, 1998; Raz *et al.*, 2001; Brown, 2007; Giannicola *et al.*, 2010). A few studies have investigated neuromodulation due to HFS in NAcc for OCD treatment, showing either the accumbal HFS provoked animal behaviour changes or local field potential changes in the limbic system due accumbal HFS (McCracken & Grace, 2007; Sesia *et al.*, 2010; Ewing & Grace, 2012).

In this study, we investigated the effects of low-frequency stimulation (LFS) and HFS on the nucleus accumbens by characterizing spontaneous neuronal electrophysiological signals before and during stimulation. Electrical stimulations and electrophysiology recordings were performed simultaneously in rat brain slices by using multi-electrode arrays (MEAs). The low-impedance microelectrodes in these arrays bias recording selectivity towards large neurons in the accumbens area. The key finding of this research is that during HFS (140 Hz) the spontaneous neuronal firing rate is suppressed to 62% of basal (no stimulation), whereas LFS (10 Hz) does not change the spontaneous neuronal firing rate. Both HFS and LFS have no effect on neuronal firing pattern or on neuronal oscillation synchrony. The HFS-induced direct inhibitory effect can be reversed by blocking $GABA_B$ receptors, but stays when $GABA_A$ receptors are antagonized. We suggest that this observation most likely concerns NAcc acetylcholine (ACh) interneurons as both muscarinic ACh autoreceptors and small-conductance calcium-dependent potassium (SK) channels are identified pharmacologically in the recorded neurons. We propose that HFS directly reduces the activity of accumbal cholinergic interneurons by enhancing GABA release in the stimulated region. GABA then acts through $GABA_B$ receptors on these interneurons. Potentially, suppressed ACh interneurons decrease the disinhibiting function of accumbal medium-sized spiny neurons (MSNs) in the striato-thalamocortical circuit. This finding might give an indication of the mechanism of the therapeutic effect of HFS in NAcc on restoring the abnormal hyperactive prefrontal cortex status in OCD.

Materials and methods

Brain slice preparation

Male Wistar rats (150–250 g) were deeply anaesthetized with isoflurane and then decapitated, and brains were removed rapidly and coarsely dissected in an ice-cold cutting solution (contents in mM: NaCl 124.0, KCl 3.3, $CaCl_2.2H_2O$ 2.5, $NaHCO_3$ 20.0, D-glucose 10.0, KH_2PO_4 1.2, $MgSO_4.\&H_2O$ 2.55, ascorbic acid 1.0, aerated with 95% O_2, 5% CO_2, pH 7.4) (Egert *et al.*, 2002; Kamal *et al.*, 2010; Stegenga & Heida, 2010). Coronal NAcc slices of 300 μm thickness were obtained by vibratome slicing (Vibrating blade microtome VT1000 S; Leica, Wetzlar, Germany). The NAcc was identified by its stereotaxic coordinates and its oval shape displaying the anterior commissure (white matter) in its centre, and the caudate putamen contacting dorsally. Tissue surrounding the NAcc region was removed with a fine scalpel, and the slices were sequentially transferred and stored in artificial cerebrospinal fluid (aCSF contents in mM: NaCl 124.0, KCl 3.3, $CaCl_2.2H_2O$ 2.5, $NaHCO_3$ 20.0, D-glucose 10.0, KH_2PO_4 1.2, $MgSO_4.7H_2O$ 1.3, aerated with 95% O_2, 5% CO_2, pH 7.4) at room temperature (25 °C) (Stegenga & Heida, 2010). All animal handling and preparations were conducted according to Dutch law (as stated in *Wet op de dierproeven*), and approved by DEC, the Dutch Animal Use Committee.

Electrodes and electrophysiological recording protocol

Neuronal electrophysiological activity was detected and recorded with three-dimensional MEAs (MEA60-200-3D; Qwane Biosciences S.A., Lausanne, Switzerland) which are composed of 60 platinum electrodes on the surface of a carrier substrate. The electrodes are arranged in an 8 × 8 matrix, 200 μm apart from each other (centre to centre), leaving four corner positions empty. Each cone-shaped electrode has a 40-μm-diameter base and is 40 μm high, featuring an electrical impedance of 200 kΩ at 1 kHz. A recording chamber is formed by fusing a glass ring (ø 20 mm) to the substrate plane (Heuschkel *et al.*, 2002). A titanium wire was placed within the medium chamber, which was used as a reference electrode. Brain slices were transferred to the aCSF-filled MEA chamber that was positioned on top of a heating pad, and the NAcc region was positioned on top of the electrode matrix under visual control with an inverted microscope. We used a fine nylon mesh (200-μm grid) to manually press the brain slice on the electrodes to provide a better tissue–electrode contact. Fresh aCSF was continuously perfused (3–4 mL/min) through the chamber during the whole experiment. The temperature of the aCSF in the MEA chamber was around 32 °C measured by a thermometer during the experiments.

Signals from the 60 electrodes were preamplified (gain: 1000), band-pass filtered (10–10 000 Hz) with a 60-channel preamplifier (MEA1060-Inv-BC; Multi Channel Systems, Reutlingen, Germany), and sampled at 16 kS/s with a 12-bit analog-to-digital converter (ADC, National Instruments, Austin, TX, USA). By taking advantage of the blanking circuit within the MEA preamplifier, neuronal signals were recorded continuously even when the electrical stimulus was applied, during which stimulation artefacts were consequently blocked. Online data monitoring was performed with a customized Labview program (National Instruments), and all acquired data were offline processed in Matlab (Mathworks, Natick, MA, USA). Within the online monitoring program, neuronal action potentials were detected by thresholding the filtered neuronal signals (400–4000 Hz). In addition to the unfiltered neuronal signals, we also stored action potential segments. The action potential segments were stored when their amplitude exceeded the threshold which is five times of the root mean square (RMS) value (typically 2–3 μV in this experimental set-up).

Stimulation protocol

Monopolar biphasic stimulations were applied in this study. One electrode was selected from the 60-electrode array as stimulation site. This site was chosen for its position within the NAcc region, regardless of distinguishing the shell or core region. The utilized stimulus consisted of biphasic negative-then-positive current pulse trains (phase amplitude ± 65 μA, phase duration 100 μs), implemented in an a-priori chosen stimulation frequency (2–140 Hz) (Wagenaar *et al.*, 2004; Li

et al., 2006). The charge balance current pulse was chosen to avoid electrode saturation during long (up to 6 min) high-frequency stimulation (based on the observation from preliminary experiments, not published data). After 2–3 min baseline (stimulus-free) recording, stimulation was applied at a frequency of 140 Hz (HFS) or 10 Hz (LFS) for 200 s each in a randomized order (Benabid *et al.*, 1987, 2005).

Pharmacology

Apamin (100 nM; 178270, Merck Millipore, Darmstadt, Germany) was applied to specifically block SK channels. Atropine (1 μM; A0132, Sigma-Aldrich, St Louis, MO, USA) was used to block muscarinic ACh receptors. (−)-Bicuculline methochloride (100 μM; B7686, Sigma-Aldrich) or 50 μm picrotoxin (P1675; Sigma-Aldrich) was chosen to block $GABA_A$ receptor-associated Cl^- currents. Carbachol (10 μM; Merck Millipore) was applied to activate muscarinic ACh receptors. CGP7930 (5 μM; Merck Millipore) was used to block $GABA_B$ receptors. The wash-in time was set to at least 400 s and the washout time was set to at least 600 s.

Data analysis

Data analysis was performed using a custom-made program running under the Matlab (MathWorks) environment. The neuronal electrophysiological properties were interpreted by discharge shape, firing rate and firing pattern. Neural discharge shapes were classified by using a principal component analysis and expectation maximization algorithm (Lewicki, 1998). Neuronal discharge density histograms with 5-s bin size were calculated. Based on these histograms, firing patterns were classified into three types, regular, bursty and random (Kaneoke & Vitek, 1996; Stegenga & Heida, 2010). Spike train autocorrelation histograms and cross-correlation histograms were calculated for delay from −1000 to 1000 ms with 10-ms bin size and were smoothed by applying a Gaussian curve (σ = 2 ms) convolution (Raz *et al.*, 1996). Peaks in auto-correlograms indicate single neuron oscillation activities, while cross-correlograms give the synchronization properties between the correlated neuron pair. Unpaired Student's *t*-test was used with GraphPad for statistical analysis.

Results

Steady spontaneous neuronal firing activities were observed from 134 active recording sites in 21 rats. The action potentials usually discharged single spikes with a biphasic waveform: a steep falling phase followed by a gently rising phase, displaying a peak to peak amplitude of 35 ± 5 μV (mean ± SEM) (Fig. 1c). As each recording site presented only one predominant action potential wave shape, we assume that the signal from each active recording site is generated from one single neuron (Harris *et al.*, 2000; Segev *et al.*, 2004). Electrophysiological signals analysed in this work frame were collected from all accessible spontaneous firing neurons within the NAcc, without immunohistochemically or cytoarchitecturely discriminating a specific neuronal cell type (Fig. 1a).

Electrical stimulation effects on spontaneous neuronal firing activities

Mean firing rates before and during stimulation were calculated and analysed statistically based on 80 recordings of accumbal neurons from 14 rats. Figure 2a shows an example of the mean firing rate of a single neuron with respect to the stimulation frequency. The average mean baseline firing rate from these neurons was 1.19 ± 0.12 (mean ± SEM). Eight neurons were examined only under HFS 140 Hz, while the other 72 neurons were tested under both HFS 140 Hz and LFS 10 Hz stimulation. During HFS 140 Hz, 97.5% (78 of 80) of the total number of neurons had a decreased mean firing rate compared with the baseline (stimulation-free) level; the remaining neurons showed around 10% increases from baseline activities. During LFS (10 Hz), none of these 72 neurons showed either decreased or increased firing rate. The mean normalized (to baseline) firing rate during LFS 10 Hz was 1.07 ± 0.03 (mean ± SEM, n = 72), while the firing rate during 140 Hz stimulation was 0.62 ± 0.01 (mean ± SEM, n = 78), yielding a statistically significant decrease ($P < 0.05$, n = 72) (Fig. 2b). Interspike interval (ISI) histograms shown in Fig. 2c suggest that there is no significant change in neuronal firing pattern under different conditions.

As the MEA used gives us access to multiple simultaneously recorded neurons, we were able to identify eight groups of simultaneously recorded neurons in this study. Four of them contained two paired neurons, three contained three neurons, and one contained four simultaneously recorded neurons. Autocorrelation histograms were not altered by either HFS or LFS indicating neither HFS nor LFS influenced the neuronal firing patterns. The cross-correlation histograms did not demonstrate any synchronized oscillation between neuron pairs, and these were not affected by either HFS or LFS. Figure 3 gives a sample of three simultaneously recorded neurons.

GABA receptors' roles in electrical stimulation-induced neuronal responses

As mentioned before, the high-frequency electrical stimulation-provoked neuronal inhibition is probably mediated by activated GABA receptors on the stimulated neurons subsequent to selective HFS-induced GABA release (Feuerstein *et al.*, 2011). We identified the GABA receptor-mediated neuronal inhibition by applying bicuculline or picrotoxin to block $GABA_A$ receptors, and CGP to block $GABA_B$ receptors, respectively.

Bicuculline blocks $GABA_A$ receptors, but does not affect the influence of HFS or LFS

Bicuculline perfusion was performed in 10 brain slices, administered to the perfusate after one set of HFS and LFS. The drug remained present for around 30 min. A total of 31 neurons with continuous and spontaneous firing activity were analysed in this session. Figure 4a shows that the mean firing rate of a single neuron is being altered during HFS and LFS in both pre- and post-bicuculline administration states. In general, the mean firing rate (calculated from 200-s recording segments) dropped during HFS but stayed steady during LFS in both the absence and the presence of bicuculline. In total, 83% of neurons (10 of 12) showed inhibited mean firing rates (> 30% decrease) by HFS, but were not affected (< 10% decrease) by LFS when bicuculline was absent; while under bicuculline superfusion 75% of the neurons (9 of 12) had a suppressed mean firing rate induced by HFS. In short, the mean firing rate was significantly inhibited by HFS when bicuculline was either absent or present ($P < 0.0001$, n = 31), as shown in Fig. 4d.

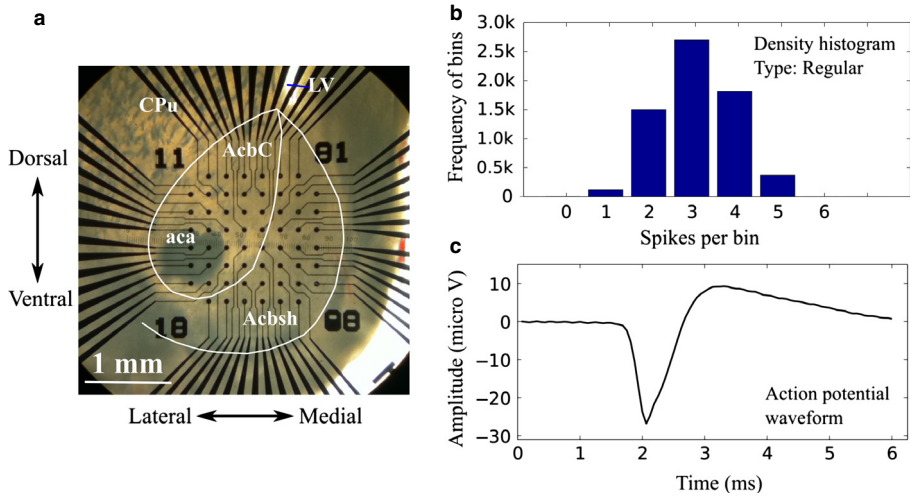

FIG. 1. (a) Image of a rat's coronal brain slice on top of a three-dimensional MEA, kept in position by a nylon mesh. White lines schematically indicate AchC, AchSh, caudate putamen (CPu) and anterior commissure area (aca) (Paxinos & Watson, 2005). (b) The major neuronal discharge pattern in this study is regular. The discharge density histogram plots the number of bins (bin size 1 s) on the *y*-axis which contain a certain number of spikes (*x*-axis). The *x*-axis displays values from zero, meaning there is no spike within a 1-s bin, to the value given by the maximal number of spikes within 1 s. The density histogram in this figure shows a symmetrical normal distribution indicating a regular firing pattern (Kaneoke & Vitek, 1996). (c) An averaged single unit action potential waveform recorded from one electrode located in the accumbal region. The peak to peak amplitude reaches about 40 μV, with a discharging period around 1.5 ms.

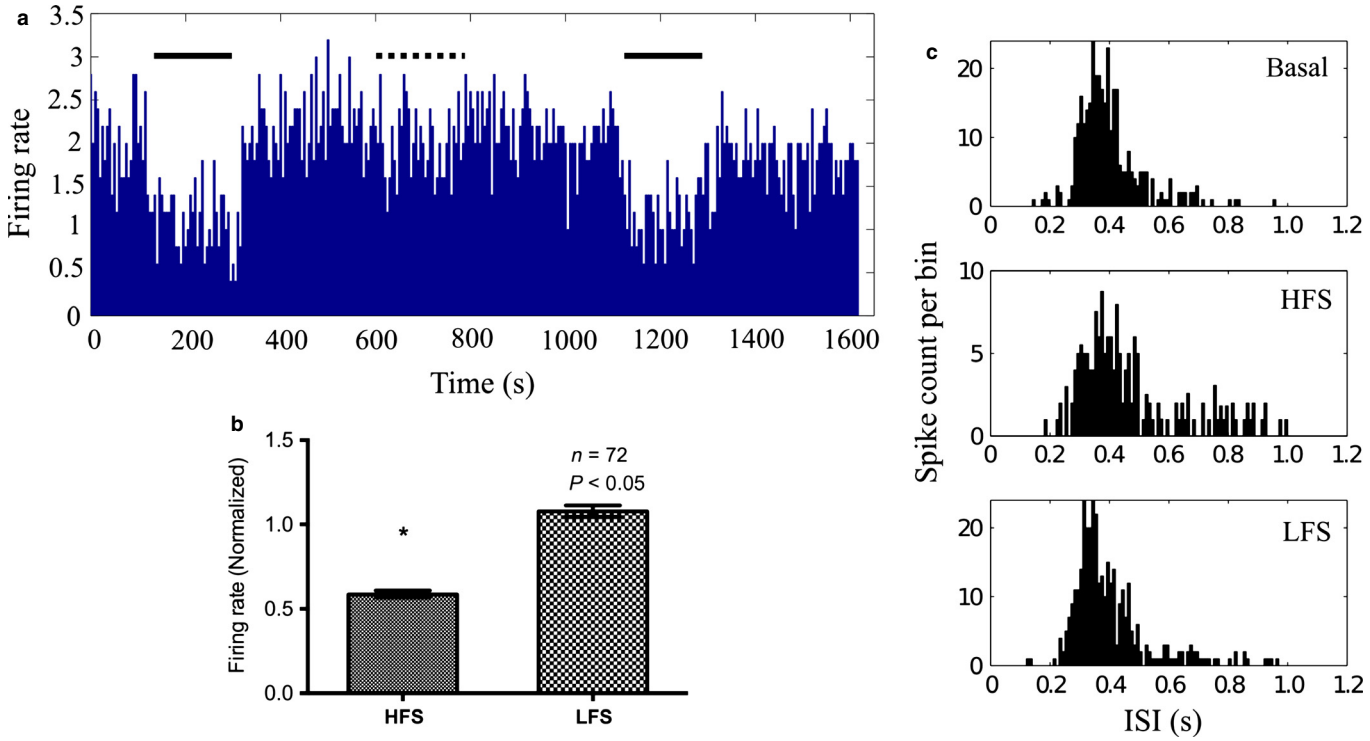

FIG. 2. (a) Firing rate histogram showing periods of neuronal spontaneous activity, and periods in which HFS and LFS are applied. Solid lines indicate HFS at 140 Hz and dashed line indicates LFS at 10 Hz. The firing rate is suppressed profoundly during HFS, but is not affected by LFS. (b) The overall mean firing rates during HFS and LFS are calculated by averaging the firing rates of 72 neurons in 14 rats, and normalized to the baseline firing rate. A significant difference is found using the unpaired *t*-test (*$P < 0.05$, $n = 72$). Data are mean ± SEM. (c) ISI histograms of a single neuron of basal, HFS and LFS conditions, indicating firing pattern does not change significantly during different stimulation conditions. Bin size is 10 ms.

Picrotoxin blocks $GABA_A$ receptors, but does not affect the influence of HFS or LFS

Five brain slices were measured under picrotoxin perfusion, and the drug was washed in for at least 5 min and remained present for 20 min to allow one set of HFS and LFS to be applied. Twenty neurons with continuous and spontaneous firing activity were analysed. In Fig. 4b, the averaged firing rate over time of one neuron examined with HFS and LFS in the presence of picrotoxin is shown. Similar to the effect of the bicuculline perfusion, the firing rate was diminished by HFS but not affected by LFS in general. The statistical evaluation in Fig. 4d shows a significant difference

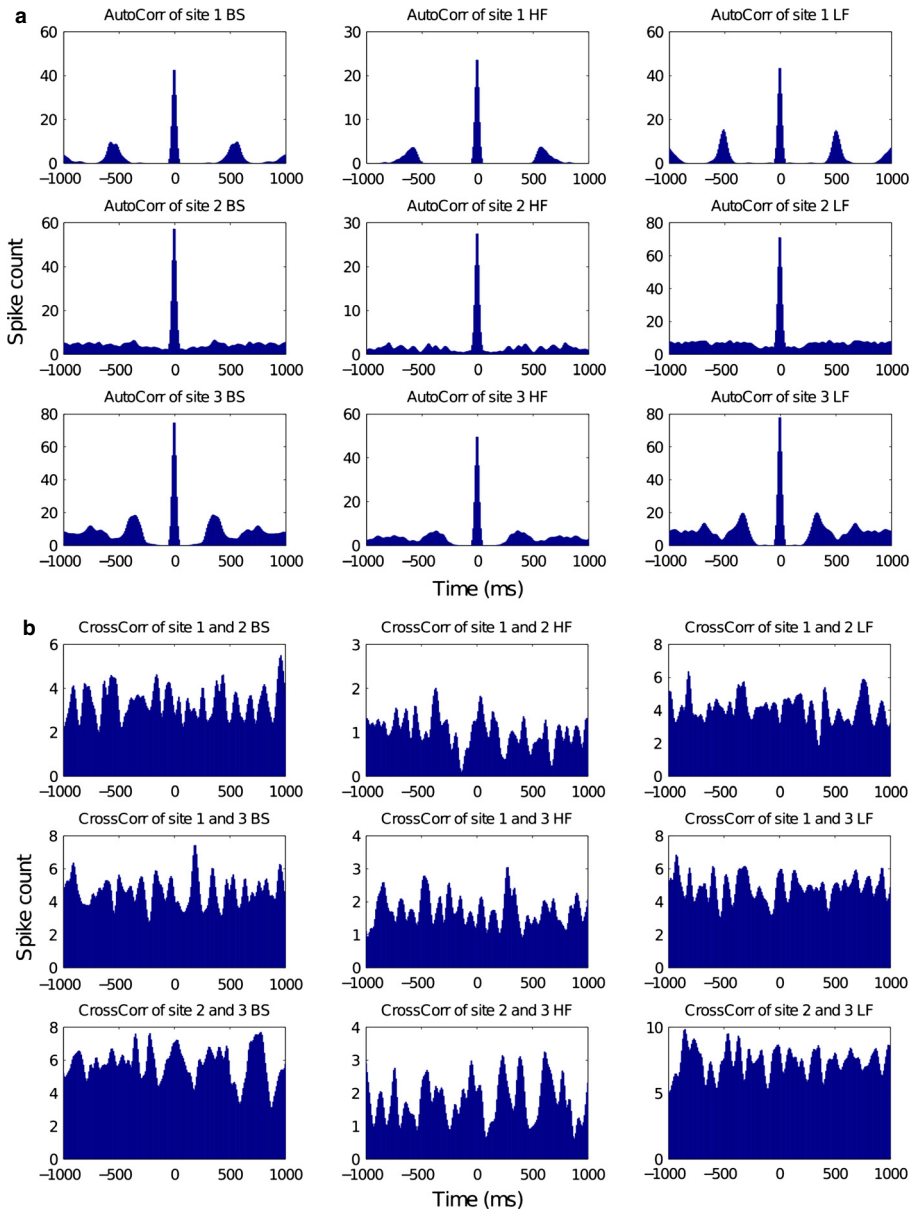

FIG. 3. Spike trains auto-correlograms (a) and cross-correlograms (b) of three simultaneously recorded neurons in control, HFS and LFS conditions. All correlation histograms were calculated for delay from −1000 to 1000 ms with 10-ms bin size, and smoothed by convoluting with Gaussian curve (σ = 2 ms). Unit 1 is found to have oscillatory activity at about 2 Hz; the other two units present no obvious oscillation properties in the auto-correlograms. From the cross-correlograms, no synchronized oscillation between these three simultaneously recorded neurons is detected. Furthermore, neither HFS nor LFS alters the auto-correlograms or the cross-correlograms.

in normalized firing rate between HFS and LFS in the presence of picrotoxin ($P < 0.0001$, $n = 20$), suggesting that $GABA_A$ receptors did not play a pronounced role in HFS-induced neuronal responses.

CGP blocks $GABA_B$ receptors, and abolishes the HFS inhibition effect

G protein coupled $GABA_B$ receptors was investigated in five brain slices with CGP perfusion. We selected the recorded neuron based on the criterion described in the preceding sections, and 26 neurons were chosen and analysed in this part. Figure 4c gives a sample firing rate moderated by HFS and LFS when CGP was perfused, illustrating that neither HFS nor LFS affects the spontaneous firing activity. In contrast to the $GABA_A$ receptor antagonists (see Fig. 4d), CGP reverted the supposedly (without drugs) inhibited neuronal firing rate due to HFS ($P = 0.1268$, $n = 26$), strongly indicating that HFS diminishes neuronal firing rate through facilitated $GABA_B$ receptors on the neurons under investigation.

Identification of neuron type

It is well known that unlike the other accumbal neurons the cholinergic interneurons fire tonically and autonomously even in the absence of synaptic inputs (Wilson *et al.*, 1990; Kawaguchi *et al.*, 1995). These so called tonically active neurons (TANs) can be

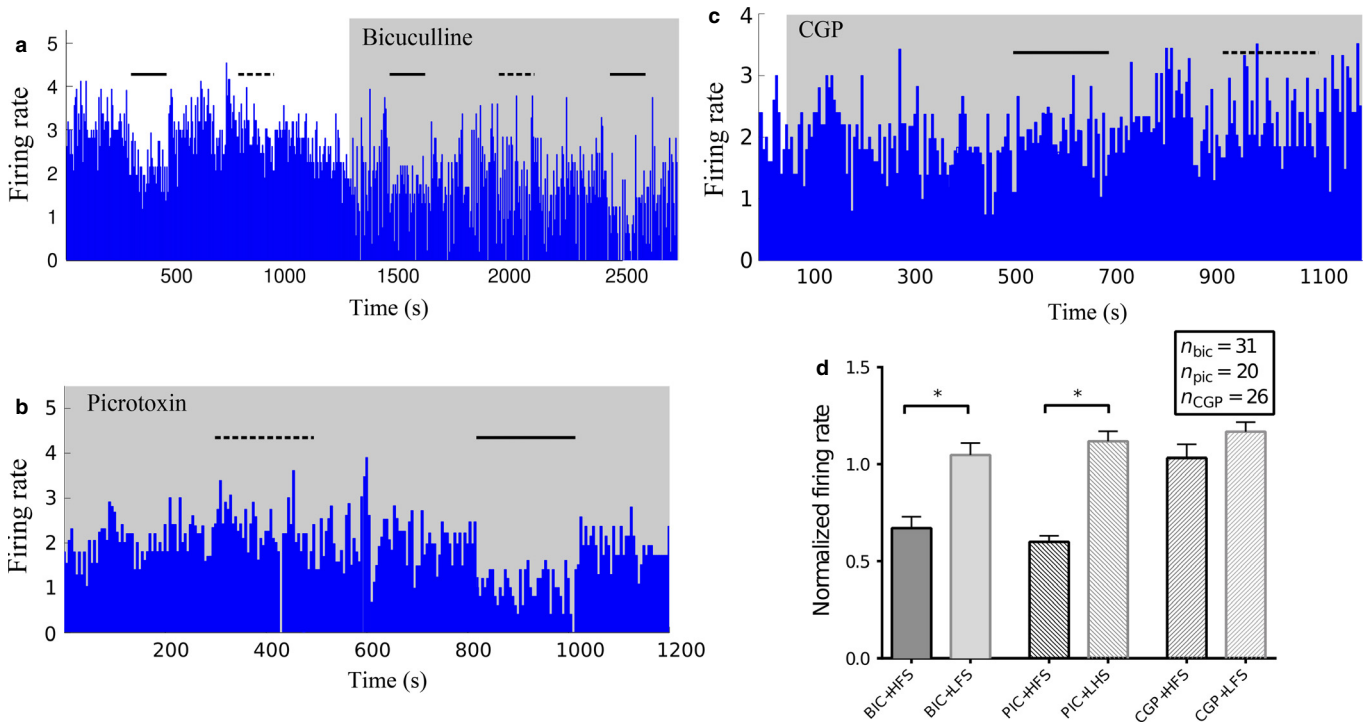

FIG. 4. (a) Modulations of the firing rate of one neuron caused by HFS and LFS with and without bicuculline present. HFS diminishes the firing rate despite the presence of bicuculline (100 μM). (b) The $GABA_A$ receptor antagonist picrotoxin (50 μM) does not have a reverting effect on HFS-induced neuronal inhibition. (c) $GABA_B$ receptor antagonist CGP (5 μM) reverts the HFS-elicited neuronal inhibition. (d) Statistical comparison of the normalized (to basal value) firing rate during HFS and LFS with bicuculline, picrotoxin and CGP present. There is a significant difference between firing rate under HFS and LFS when bicuculline is present ($n = 31$, $^*P < 0.0001$). The firing rate under HFS and LFS when picrotoxin is perfused also displays statistical significance ($n = 20$, $^*P < 0.0001$). However, the difference between the firing rate during HFS and LFS in the presence of CGP is not statistically significant ($n = 26$, $P = 0.1268$).

identified by certain pharmacological interventions such as modulating their muscarinic autoreceptors or their SK channels (Goldberg & Wilson, 2005).

Muscarinic autoreceptors

Twenty neurons with tonic and autonomous firing pattern were perfused with carbachol, a non-selective cholinergic agonist that binds to all muscarinic receptor subtypes (M1–M5). Sixteen of 20 neurons presented a more than 30% decrease in their spontaneous firing rate in the presence of carbachol (Fig. 5a2). For six neurons with decreased firing activities due to the carbachol perfusion, we additionally added atropine (a cholinergic antagonist) to the perfusion buffer. We observed that the neuronal spontaneous firing activity recovered to the basal activity after atropine was administered. Figure 5a1 illustrates the firing rate over time from a single neuron, evidently demonstrating that the neuronal firing activity is suppressed by carbachol while this suppressing effect can be abolished by atropine.

Apamin induces bursty activity by selectively blocking SK channels

Apamin was chosen to selectively bind to the SK channel, which represents the key to switch the spontaneous firing pattern of the accumbal cholinergic interneuron from regular to bursty (Bennett & Wilson, 1999; Goldberg & Wilson, 2005). Apamin perfusion was performed in two brain slices; 10 neurons fired autonomously, regularly and in a single spike pattern before apamin was introduced to the slice, while six of them changed to rhythmic bursty firing when apamin was administered. From the modulation of the firing rate of a single neuron (Fig. 5b1), a transition on the firing pattern before and after apamin perfusion is noticeable and the rhythmic bursty firing is predominant during apamin presence. The ISI histograms in Fig. 5b2 also illustrate a typical symmetric normal distribution of the regular firing under basal conditions (upper graph), and two distinct separate distributions of the rhythmic bursty firing when apamin was present (lower graph).

Discussion

In the present study, we applied HFS and LFS (140 Hz, 10 Hz) to rat accumbal slices and recorded the local neuronal activity before, during and after the stimulation. This is the first study, to our knowledge, that has monitored and analysed neuronal spontaneous activities in the stimulated brain area while HFS or LFS was applied simultaneously. Results show a significant decrease in spontaneous neuronal activity only during HFS, which is postulated to be induced by either membrane depolarization blockade or selective local GABA release (Dostrovsky *et al.*, 2000; Beurrier *et al.*, 2001; Filali *et al.*, 2004; Feuerstein *et al.*, 2011). Neuronal firing pattern or oscillation synchrony is not affected by either HFS or LFS. The $GABA_A$ receptor antagonist bicuculline and picrotoxin, and the $GABA_B$ receptor antagonist CGP were tactically applied to oppose GABA transmission. Interestingly, blocking $GABA_A$ receptors failed to affect the HFS-provoked neuronal inhibition. In contrast, the suppressed $GABA_B$ transmission abolished HFS-induced neuron inhibition and brought the neuronal firing rate back to basal levels. Carbachol diminished neuronal spontaneous firing while adding

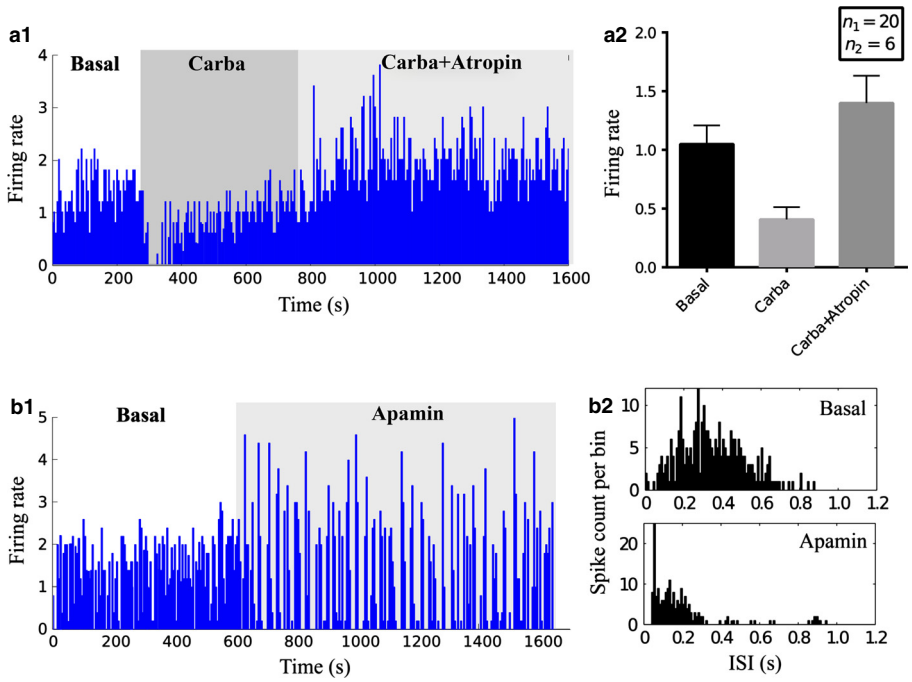

FIG. 5. (a1) Carbachol opposes the neuron spontaneous firing and this effect is abolished when atropine is administered. Statistical analysis is shown in (a2), obtained from 20 neurons analysing the effect of carbachol and six neurons for carbachol + atropine. (b1) Apamin provokes a pronounced bursty firing on the autonomously firing neuron. (b2) ISI histogram of the basal status illustrating a typical symmetrical normal distribution (regular firing pattern), and two distinct separate distributions of rhythmic bursty firing when the apamin was present. Bin size is 10 ms.

atropine compensated for the carbachol effect and took the neuronal firing rate back to normal.

Effect of electrical stimulation on spontaneous firing

According to Feuerstein *et al.* (2011), HFS selectively induces action potentials in GABAergic axons and leads to GABA release from axon terminals. Orthodromic action potentials in GABAergic neurons are consequently releasing GABA to reach the somatodendrites of ACh neurons, probably through metabotropic $GABA_B$ receptors, which is supported by our findings (Fig. 4d). GABA released onto (postsynaptic) somatodendritic $GABA_B$ heteroreceptors of ACh interneurons then activate these heteroreceptors to decrease the tonic firing rate of ACh interneurons.

Neuron type

In NAcc, the GABAergic MSNs (size 10–20 μm) contribute the vast majority of up to 95% accumbal neurons. The MSNs are relay neurons both in the mesolimbic pathway and in the cortico-basal-thalamo-cortical loops (Fig. 6b) (Heimer *et al.*, 1991; O'Donnell & Grace, 1995). Minority populations in NAcc are aspiny interneurons which can be categorized anatomically to medium-sized GABAergic interneurons and large cholinergic interneurons (Tepper & Bolam, 2004). Although those interneurons are much lower in number than the MSNs, they play a disproportionally critical function in regulating the excitatory and inhibitory accumbal synaptic inputs by interfering with the postsynaptic potentials of MSNs (Jiang & North, 1991; Kawaguchi *et al.*, 1995; Brundege & Williams, 2002).

It is widely believed that the large aspiny cholinergic interneurons are TANs, which fire autonomously and steadily at a low frequency (1–9 Hz) (Wilson & Groves, 1981; Wilson *et al.*, 1990; Aosaki *et al.*, 1995; Inokawa *et al.*, 2010; Goldberg & Reynolds, 2011). In our experiments, neuronal action potentials were autonomously and steadily (up to 70 min) generated at a mean frequency of 1.19 Hz, despite the lack of synaptic input from cortex and midbrain structures in these isolated accumbal slices, evidently suggesting that the recorded neurons are potentially cholinergic interneurons. Based on this assumption, we applied carbachol to the slices to facilitate the muscarinic ACh receptors; atropine was used to antagonize these receptors. The muscarinic autoreceptor M4 is predominately expressed in striatal cholinergic interneurons, and when activated it diminishes Ca^{2+} channel opening and increases K^+ channel opening; it therefore elicits membrane hyperpolarization and suppresses the cholinergic neuron activity. As expected, in our experiments carbachol diminished the neuronal firing rate, whereas atropine abolished this inhibition, compellingly implying that the recorded neurons are cholinergic interneurons.

Cholinergic interneurons exhibit two major spontaneous firing patterns in slices, one is single spiking and the other is rhythmic bursting (Bennett & Wilson, 1999). These firing patterns are regulated by potassium currents that give rise to two respective types of after-hyperpolarizations (AHPs). In the single spiking pattern, the apamin-sensitive (SK) current (I_{SK}) is dominant and generates a prominent medium-sized AHP (mAHP) following each action potential, while the rhythmic bursting pattern is built up by a calcium-induced calcium-release (CICR)-activated long-lasting slower AHP (sAHP). By applying apamin to cholinergic neurons, the apamin-sensitive calcium-dependent potassium current is abolished. Consequently, it reduces mAHP after each single spike and raises sAHP, therefore interrupting single spiking and triggering bursts (Goldberg & Wilson, 2005). The bursty activities of the recorded neurons that are elicited by apamin administration in our study are probably derived from the abolished I_{SK}, implying that the recorded neurons are cholinergic interneurons.

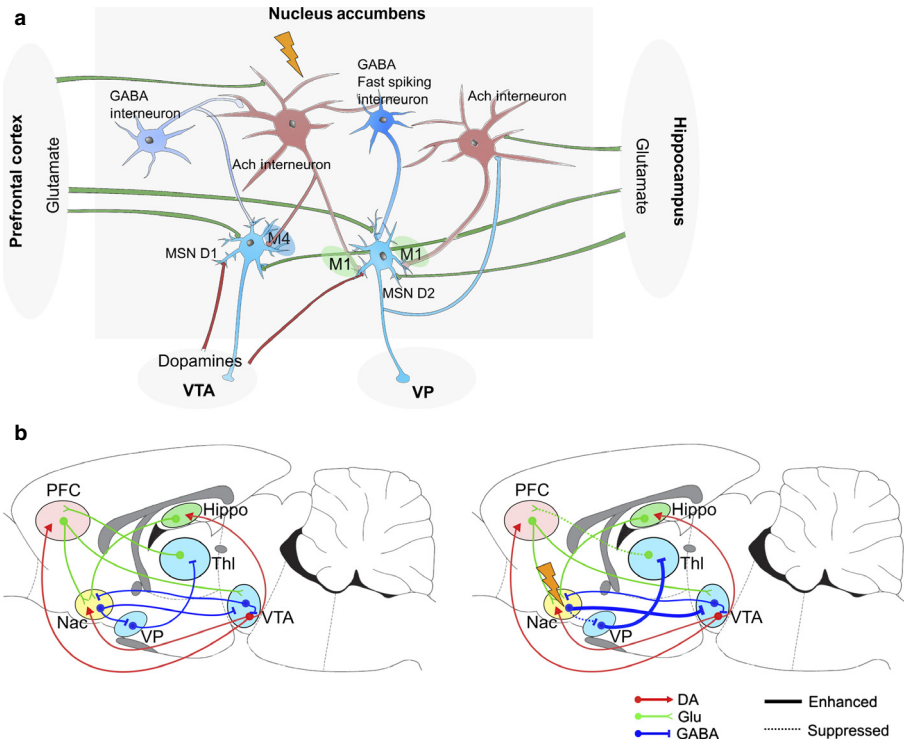

FIG. 6. (a) In the NAcc, MSNs containing enkephalin (ENK)/GABA and D_2 receptors mainly project to the ventral pallidum (VP), and the substance P (SP)/GABA MSNs expressing D_1 receptors project to the ventral tegmental area (VTA). The cholinergic interneurons act on accumbo-nigral SP/GABA neurons mainly through inhibitory muscarinic M_4 receptors, and on accumbo-pallidal ENK/GABA neurons through facilitatory M_1 receptors. In addition, striatal ACh interneurons are capable of provoking glutamatergic EPSPs on the neighbouring MSNs according to optogenetic findings (Higley *et al.*, 2011). (b) Left: sketch of the neuron network illustrating the brain structures and neurotransmitters that are probably involved in OCD pathology development. Right: when applying HFS to the NAcc, we propose that the tonically spontaneous firing of ACh neurons is suppressed by a reduction of the mean firing rate. Thus, the disinhibitory function of the ventral pallidum is decreased through less stimulation of the facilitatory M_1 receptors on accumbal MSNs. The more inhibited ventral median thalamus nucleus therefore releases less glutamate in the prefrontal cortex.

Implication

MSNs containing enkephalin (ENK)/GABA and D_2 receptors mainly project to the ventral pallidum, and substance P (SP)/GABA MSNs expressing D_1 receptors project to the ventral tegmental area (Heimer *et al.*, 1991; Brog *et al.*, 1993). The cholinergic interneurons act on accumbo-nigral SP/GABA MSNs mainly through inhibitory muscarinic M_4 receptors, and on accumbo-pallidal ENK/GABA MSNs through facilitatory M_1 receptors (see Fig. 6a) (Di Chiara *et al.*, 1994). In addition, according to the optogenetic findings, striatal ACh interneurons are capable of mediating fast glutamatergic transmission and triggering excitatory postsynaptic potentials on the neighbouring striatal output neurons (namely MSNs) (Higley *et al.*, 2011). Figure 6b shows a sketch of a neuron network illustrating the brain structures and neurotransmitters that potentially are involved in OCD pathology development (Aouizerate *et al.*, 2004b; Rauch *et al.*, 2006). When giving HFS to the NAcc, we propose that the tonically spontaneous firing of ACh interneurons is disturbed by reducing the mean firing rate. Therefore, there is less stimulation of the facilitatory M_1 receptors on accumbal MSNs. The reduced action potential firing of accumbo-pallidal MSNs reduces the inhibition of target neurons in the ventral pallidum. A more inhibited ventral median thalamus nucleus therefore results in less glutamate release in the prefrontal cortex. This might be one of the mechanisms underlying the therapeutic effects of HFS on reducing the abnormally hyperactive prefrontal cortex function.

Indeed, ACh interneurons are not the only neurons that become stimulated in this study, with the abundant projection MSNs also being affected by the electrical stimulation protocol. However, MSNs do not fire spontaneously or steadily to allow us to perform a thorough investigation on the effects of HFS and LFS on their electrophysiological properties, so we cannot infer potential influences elicited by the stimulated MSNs. Furthermore, we are aware that the spread of the stimulation field within a thin slice will be different compared with stimulation within the brain. However, the exact extent of the stimulation field within the human brain is also not fully known and in for voltage-controlled stimulation, this field may be influenced significantly by the resistive gliosis encapsulation around the electrode (Lempka *et al.*, 2009). Nevertheless, the main goal of this study is to identify the response of a specific type of neuron to electrical stimulation as a first step in revealing the mechanisms that may underlie the effectiveness of DBS in NAcc.

Acknowledgements

We thank the Graduate School for Computing in Medicine and Life Sciences funded by Germany Excellence Initiative [DFG GSC 235/1] for supporting Y.X. We thank Bettie Klomphaar for the animal preparation work. The authors declare that the research was conducted in the absence of any commercial or financial relationships that could be construed as a potential conflict of interest.

Abbreviations

ACh, acetylcholine; aCSF, artificial cerebrospinal fluid; AHP, after-hyperpolarization; DBS, deep brain stimulation; GABA, γ-amino-butyric acid; HFS, high-frequency stimulation; ISI, interspike interval;

LFS, low-frequency stimulation; MEA, multi-electrode array; MSN, medium spiny neuron; NAcc, nucleus accumbens; OCD, obsessive-compulsive disorder; SK, small-conductance calcium-dependent potassium; SP, substance P; TAN, tonically active neuron.

References

Aosaki, T., Kimura, M. & Graybiel, A.M. (1995) Temporal and spatial characteristics of tonically active neurons of the primate's striatum. *J. Neurophysiol.*, **73**, 1234–1252.

Aouizerate, B., Cuny, E., Martin-Guehl, C., Guehl, D., Amieva, H., Benazzouz, A., Fabrigoule, C., Allard, M., Rougier, A., Bioulac, B., Tignol, J. & Burbaud, P. (2004a) Deep brain stimulation of the ventral caudate nucleus in the treatment of obsessive-compulsive disorder and major depression. *J. Neurosurg.*, **101**, 682–686.

Aouizerate, B., Guehl, D., Cuny, E., Rougier, A., Bioulac, B., Tignol, J. & Burbaud, P. (2004b) Pathophysiology of obsessive–compulsive disorder, a necessary link between phenomenology, neuropsychology, imagery and physiology. *Prog. Neurobiol.*, **72**, 195–221.

Benabid, A.L., Pollak, P., Louveau, A., Henry, S. & de Rougemont, J. (1987) Combined (thalamotomy and stimulation) stereotactic surgery of the vim thalamic nucleus for bilateral parkinson disease. *Appl. Neurophysiol.*, **50**, 344–346.

Benabid, A.L., Pollak, P., Hoffmann, D., Gervason, C., Hommel, M., Perret, J.E., de Rougemont, J. & Gao, D.M. (1991) Long-term suppression of tremor by chronic stimulation of the ventral intermediate thalamic nucleus. *Lancet*, **337**, 403–406.

Benabid, A.L., Wallace, B., Mitrofanis, J., Xia, R., Piallat, B., Chabardes, S. & Berger, F. (2005) A putative generalized model of the effects and mechanism of action of high frequency electrical stimulation of the central nervous system. *Acta Neurol. Belg.*, **105**, 149–157.

Bennett, B.D. & Wilson, C.J. (1999) Spontaneous activity of neostriatal cholinergic interneurons in vitro. *J. Neurosci.*, **19**, 5586–5596.

Bergman, H., Feingold, A., Nini, A., Raz, A., Slovin, H., Abeles, M. & Vaadia, E. (1998) Physiological aspects of information processing in the basal ganglia of normal and parkinsonian primates. *Trends Neurosci.*, **21**, 32–38.

Beurrier, C., Bioulac, B., Audin, J. & Hammond, C. (2001) High-frequency stimulation produces a transient blockade of voltage-gated currents in subthalamic neurons. *J. Neurosci.*, **85**, 1351–1356.

Brog, J.S., Salyapongse, A., Deutch, A.Y. & Zahm, D.S. (1993) The patterns of afferent innervation of the core and shell in the "accumbens" part of the rat ventral striatum: immunohistochemical detection of retrogradely transported fluoro-gold. *J. Comp. Neurol.*, **338**, 255–278.

Brown, P. (2007) Abnormal oscillatory synchronisation in the motor system leads to impaired movement. *Curr. Opin. Neurobiol.*, **17**, 656–664.

Brundege, J.M. & Williams, J.T. (2002) Differential modulation of nucleus accumbens synapses. *J. Neurophysiol.*, **88**, 142–151.

Di Chiara, G., Morelli, M. & Consolo, S. (1994) Modulatory functions of neurotransmitters in the striatum: ACh/dopamine/NMDA interactions. *Trends Neurosci.*, **17**, 228–233.

Dostrovsky, J.O., Levy, R., Wu, J.P., Hutchison, W.D., Tasker, R.R. & Lozano, A.M. (2000) Microstimulation-induced inhibition of neuronal firing in human globus pallidus. *J. Neurophysiol.*, **84**, 570–574.

Egert, U., Heck, D. & Aertsen, A. (2002) Two-dimensional monitoring of spike networks in acute brain slices. *Exp. Brain Res.*, **142**, 268–274.

Ewing, S.G. & Grace, A.A. (2012) Long-term high frequency deep brain stimulation of the nucleus accumbens drives time-dependent changes in functional connectivity in the rodent limbic system. *Brain Stimul.*, **6**, 274–285.

Feuerstein, T.J., Kammerer, M., Lücking, C.H. & Moser, A. (2011) Selective GABA release as a mechanistic basis of high frequency stimulation used for the treatment of neuropsychiatric diseases. *N.-S. Arch. Pharmacol.*, **384**, 1–20.

Filali, M., Hutchison, W., Palter, V., Lozano, A. & Dostrovsky, J. (2004) Stimulation-induced inhibition of neuronal firing in human subthalamic nucleus. *Exp. Brain Res.*, **156**, 274–281.

Giannicola, G., Marceglia, S., Rossi, L., Mrakic-Sposta, S., Rampini, P., Tamma, F., Cogiamanian, F., Barbieri, S. & Priori, A. (2010) The effects of levodopa and ongoing deep brain stimulation on subthalamic beta oscillations in Parkinson's disease. *Exp. Neurol.*, **226**, 120–127.

Goldberg, J.A. & Reynolds, J.N.J. (2011) Spontaneous firing and evoked pauses in the tonically active cholinergic interneurons of the striatum. *Neuroscience*, **198**, 27–43.

Goldberg, J.A. & Wilson, C.J. (2005) Control of spontaneous firing patterns by the selective coupling of calcium currents to calcium-activated potassium currents in striatal cholinergic interneurons. *J. Neurosci.*, **25**, 10230–10238.

Gross, R.E. (2004) Deep brain stimulation in the treatment of neurological and psychiatric disease. *Expert Rev. Neurother.*, **4**, 465–478.

Harris, K.D., Henze, D.A., Csicsvari, J., Hirase, H. & Buzsa′ki, G. (2000) Accuracy of tetrode spike separation as determined by simultaneous intracellular and extracellular measurements. *J. Neurophysiol.*, **84**, 401–414.

Heimer, L., Zahm, D.S., Churchill, L., Kalivas, W. & Wohltmann, C. (1991) Specificity in the projection patterns of accumbal core and shell in the rat. *Neuroscience*, **41**, 89–125.

Heuschkel, M.O., Fejtl, M., Raggenbass, M., Bertrand, D. & Renaud, P. (2002) A three-dimensional multi-electrode array for multi-site stimulation and recording in acute brain slices. *J. Neurosci. Meth.*, **114**, 135–148.

Higley, M.J., Gittis, A.H., Oldenburg, I.A., Balthasar, N., Seal, R.P., Edwards, R.H., Lowell, B.B., Kreitzer, A.C. & Sabatini, B.L. (2011) Cholinergic interneurons mediate fast VGluT3-dependent glutamatergic transmission in the striatum. *PLoS One*, **6**, e19155.

Huff, W., Lenartz, D., Schormann, M., Lee, S.H., Kuhn, J., Koulousakis, A., Mai, J., Daumann, J., Maarouf, M., Klosterkötter, J. & Sturm, V. (2010) Unilateral deep brain stimulation of the nucleus accumbens in patients with treatment- resistant obsessive-compulsive disorder: outcomes after one year. *Clin. Neurol. Neurosur.*, **112**, 137–143.

Inokawa, H., Yamada, H., Matsumoto, N., Muranishi, M. & Kimura, M. (2010) Juxtacellular labeling of tonically active neurons and phasically active neurons in the rat striatum. *Neuroscience*, **168**, 395–404.

Jiang, Z.-G. & North, R.A. (1991) Membrane properties and synaptic responses of rat striatal neurons in vitro. *J. Physiol.*, **443**, 533–553.

Kamal, A., Van der Harst, J.E., Kapteijn, C.M., Baars, A.J., Spruijt, B.M. & Ramakers, G.M. (2010) Announced reward counteracts the effects of chronic social stress on anticipatory behavior and hippocampal synaptic plasticity in rats. *Exp. Brain Res.*, **201**, 641–651.

Kaneoke, Y. & Vitek, J.L. (1996) Burst and oscillation as disparate neuronal properties. *J. Neurosci. Meth.*, **68**, 211–223.

Kawaguchi, Y., Wilson, C.J., Augood, S.J. & Emson, P.C. (1995) Striatal interneurones: chemical, physiological and morphological characterization. *Trends Neurosci.*, **18**, 527–535.

Kringelbach, M.L., Jenkinson, N., Owen, S.L. & Aziz, T.Z. (2007) Translational principles of deep brain stimulation. *Nat. Rev. Neurosci.*, **8**, 623–635.

Kuhn, J., Gaebel, W., Klosterkoetter, J. & Woopen, C. (2009) Deep brain stimulation as a new therapeutic approach in therapy-resistant mental disorders: ethical aspects of investigational treatment. *Eur. Arch. Psy. Clin. N.*, **259**, 135–141.

Lempka, S.F., Miocinovic, S., Johnson, M.D., Vitek, J.L. & McIntyre, C.C. (2009) In vivo impedance spectroscopy of deep brain stimulation electrodes. *J. Neural Eng.*, **6**, 046001.

Lewicki, M.S. (1998) A review of methods for spike sorting: the detection and classification of neural action potentials. *Network-Comp. Neural.*, **9**, R53–R78.

Li, T., Thümen, A. & Moser, A. (2006) Modulation of a neuronal network by electrical high frequency stimulation in striatal slices of the rat in vitro. *Neurochem. Int.*, **48**, 83–86.

Lozano, A.M. & Lipsman, N. (2013) Probing and regulating dysfunctional circuits using deep brain stimulation. *Neuron*, **77**, 406–424.

McCracken, C.B. & Grace, A.A. (2007) High-frequency deep brain stimulation of the nucleus accumbens region suppresses neuronal activity and selectively modulates afferent drive in rat orbitofrontal cortex in vivo. *J. Neurosci.*, **27**, 12601–12610.

McIntyre, C.C., Savasta, M., Kerkerian-Le Goff, L. & Vitek, J.L. (2004) Uncovering the mechanism(s) of action of deep brain stimulation: activation, inhibition, or both. *Clin. Neurophysiol.*, **115**, 1239–1248.

O'Donnell, P. & Grace, A.A. (1995) Synaptic interactions accumbens neurons, input among excitatory afferents to nucleus hippocampal gating of prefrontal cortical. *J. Neurosci.*, **15**, 3622–3639.

Paxinos, G. & Watson, C. (2005) *The Rat Brain in Stereotaxic Coordinates*, 5th Edn. Academic Press, San Diego.

Rauch, S.L., Dougherty, D.D., Malone, D., Rezai, A., Friehs, G., Fischman, A.J., Alpert, N.M., Haber, S.N., Stypulkowski, P.H., Rise, M.T., Rasmussen, S.A. & Greenberg, B.D. (2006) A functional neuroimaging investigation of deep brain stimulation in patients with obsessive–compulsive disorder. *J. Neurosurg.*, **104**, 558–565.

Raz, A., Feingold, A., Zelanskaya, V., Vaadia, E. & Bergman, H. (1996) Neuronal synchronization of tonically active neurons in the striatum of normal and parkinsonian primates. *J. Neurophysiol.*, **76**, 2083–2088.

Raz, A., Frechter-Mazar, V., Feingold, A., Abeles, M., Vaadia, E. & Bergman, H. (2001) Activity of pallidal and striatal tonically active neurons is correlated in MPTP-treated monkeys but not in normal monkeys. *J. Neurosci.*, **21**, RC128.

Segev, R., Goodhouse, J., Puchalla, J. & Berry, M.J. (2004) Recording spikes from a large fraction of the ganglion cells in a retinal patch. *Nat. Neurosci.*, **7**, 1155–1162.

Sesia, T., Bulthuis, V., Tan, S., Lim, L.W., Vlamings, R., Blokland, A., Steinbusch, H.W.M., Sharp, T., Visser-Vandewalle, V. & Temel, Y. (2010) Deep brain stimulation of the nucleus accumbens shell increases impulsive behavior and tissue levels of dopamine and serotonin. *Exp. Neurol.*, **225**, 302–309.

Stegenga, J. & Heida, T. (2010) Oscillations in subthalamic nucleus measured by multi electrode arrays. In Bamidis, P.D., Pallikarakis, N. & Magjarevic, R. (Eds), *XII Mediterranean Conference on Medical and Biological Engineering and Computing 2010*, *vol* **29**, IFMBE Proceedings. Springer, Berlin, pp. 784–787.

Sturm, V., Lenartz, D., Koulousakis, A., Treuer, H., Herholz, K., Klein, J.C. & Klosterkötter, J. (2003) The nucleus accumbens: a target for deep brain stimulation in obsessive–compulsive- and anxiety-disorders. *J. Chem. Neuroanat.*, **26**, 293–299.

Tepper, J.M. & Bolam, J.P. (2004) Functional diversity and specificity of neostriatal interneurons. *Curr. Opin. Neurobiol.*, **14**, 685–692.

Tronnier, V.M. & Fogel, W. (2000) Pallidal stimulation for generalized dystonia. *J. Neurosurg.*, **92**, 453–456.

Wagenaar, D.A., Pine, J. & Potter, S.M. (2004) Effective parameters for stimulation of dissociated cultures using multi-electrode arrays. *J. Neurosci. Meth.*, **138**, 27–37.

Wilson, C.J. & Groves, P.M. (1981) Spontaneous firing patterns of identified spiny neurons in the rat neostriatum. *Brain Res.*, **220**, 67–80.

Wilson, C.J., Chang, H.T. & Kitai, S.T. (1990) Firing patterns and synaptic potentials of identified giant aspiny interneurons in the rat neostriatum. *J. Neurosci.*, **10**, 508–519.